A numerical simulation of the development of tropical cyclones

By LI PENG and H. L. KUO, *Department of the Geophysical Sciences, The University of Chicago, USA*

(Manuscript received April 1; revised version July 1, 1974)

ABSTRACT

A numerical experiment for the study of the development of tropical cyclones is performed with a 10-level axisymmetric model. In this model, the wind in the boundary layer is computed directly from the primitive equation of motion, but gradient balance is assumed above the boundary layer. The contribution of deep cumulus clouds to the heating of the large scale environment is parameterized along the lines of Kuo (1965) and Sundqvist (1970). The effect of the upward transport of momentum by cumulus clouds is also included in a crude manner. The experiment shows that the present model is capable of describing many features observed in real tropical cyclones. Our result differs from Sundqvist (1970) in one major aspect, namely, no rapid decay occurs after the mature stage if the external conditions and parameters remain unchanged, which is in agreement with the result of Ooyama (1969). The development process and the structure of the simulated tropical cyclone are discussed in some detail.

1. Introduction

It has long been recognized through climatological and observational studies (e.g., Palmen, 1948; Riehl & Malkus, 1961; Yanai, 1961) that *the release of latent heat by condensation* is the primary energy source for the development and maintenance of tropical cyclones. On the other hand, theoretical studies (Lilly, 1960; Kuo, 1961) have revealed and numerical experiments (e.g., Kasahara, 1961; Syono, 1962) verified that the most preferred scale of moist convection in a conditionally unstable atmosphere is of cumulus scale. Therefore, there is no doubt that the development of tropical cyclones cannot be explained without considering the interaction between cumulus clouds and the motion of the cyclone scale. The cumulus convective process unfortunately involves many complicated micro- and mesoscale mechanisms which have not yet been well understood. It is impossible to explicitly include all such micro- and mesoscale details in a tropical cyclone model even if they were perfectly known. One must find some way of parameterizing not only the contribution of the cumulus ensemble to change of the cyclone-scale flow but also the controlling effect of the cyclone-scale motion on cumulus activity. An important breakthrough to solve this difficult parameterization problem came with the studies of Kuo (1963, 1965), Ooyama (1964) and Charney & Eliassen (1964), and the proposition that the latent heat released by the cumulus convection is *proportional to the horizontal convergence* of moisture in the boundary layer given by the large scale flow, which is also equal to the upward flux of water vapor at the top of the boundary layer. Charney & Eliassen discussed the mechanism of the development of tropical cyclones from the point of view of instability which they called the conditional instability of the second kind (CISK). A major problem to implement the idea that the latent heat released by the deep cumulus is the main energy source for the tropical cyclones in a multi-level model is how this heat should be distributed vertically. Although no parameterization scheme can be completely satisfactory, a few proposed solutions can be used in the hurricane models. Thus, Kuo (1965) first proposed that the vertical distribution of the latent heat released is proportional to the temperature difference between cumulus clouds and their environment, and a rigorous derivation of this scheme is given by Kuo (1974) recently which also includes a parameterization of the influences of the shallow convection. Kuo's approach was later adopted with minor modifications by Yamasaki (1968), Rosenthal (1969) and Sundqvist (1970), and their simulated tropical cyclones agreed with reality reasonably well. Other proposed solutions are also being tested in the simulation of tropical cyclones (e.g., Rosenthal, 1973).

Tropical cyclone models are usually called balanced or unbalanced according to whether the gradient wind is assumed or not. Both categories of models possess certain advantages and disadvantages. The balanced models are certainly more restrictive than the unbalanced ones, but give less trouble in computational-stability control, and generally require less computing time. The unbalanced models can describe the real cases more closely, but they always need excessive damping to keep the computation stable. The earlier tropical cyclone models are almost exclusively balanced models. The first successful result in the numerical simulation of tropical cyclones was obtained with a balanced model by Ooyama (1964). However, in the balanced model which also assumed gradient wind balance in the boundary layer, the computed cyclone was not sufficiently realistic in several aspects, e.g., the eye tended to expand too rapidly during the mature stage. Later Ooyama (1969) abandoned the balance approximation in the calculation of the boundary layer flow. Instead, he made a diagnostic use of the steady-state primitive equation in radial direction. The results were improved. Sundqvist (1970) laso adopted a balanced model but without a separate boundary layer. The radial flow below the 900 mb level was obtained from the Stoke's stream function which in turn was the solution of the compatibility equation under the hydrostatic and gradient-wind assumptions, and, as a remedy, the potential temperature at the 900 mb level was not computed from the thermal-wind equation but interpolated from the value at 800 mb and that below 900 mb which was obtained from the first law of thermodynamics. The simulated tropical cyclone agreed quantitatively well with the observed real ones. However, an artificial smoothing was applied by Sundquist to the tangential wind field every time-step to suppress the oscillation near the center and to reduce the conspicuous irregularities in the vertical distribution.

In the present study, a numerical experiment on the development of tropical cyclones is performed with a 10-level axisymmetric model. In this model, the wind in the boundary layer is computed directly from the primitive equation of motion, but the gradient wind balance is assumed above the boundary layer. The contribution of deep cumulus convections to the heating of the large-scale environment is parameterized along the lines of Kuo (1965) and Sundqvist (1970), with the entrainment effect on cumulus clouds roughly taken into account through the computation of cloud temperature. The effect of cumulus clouds on momentum transports in the vertical is also included roughly by increasing the eddy-viscosity coefficient in an amount proportional to the cumulus activity measured by boundary layer pumping. No artificial smoothing is applied to the computed fields. The dynamic equations and the boundary conditions used in the numerical experiments are presented in section 2, the numerical methods used are discussed in section 3, while the results of the numerical experiment are discussed in some detail in section 4.

2. The numerical model

Under the assumption that the motion is axisymmetric and in hydrostatic equilibrium, the governing equations may be written in cylindrical p-coordinates as

$$\frac{\partial u}{\partial t} = -v\left(f+\frac{u}{r}\right) - v\frac{\partial u}{\partial r} - \omega\frac{\partial u}{\partial p} + K_H\left(\frac{\partial^2}{\partial r^2}+\frac{1}{r}\frac{\partial}{\partial r}-\frac{1}{r^2}\right)u + g\frac{\partial \tau_u}{\partial p} \tag{1}$$

$$\frac{\partial v}{\partial t} = u\left(f+\frac{u}{r}\right) - v\frac{\partial v}{\partial r} - \omega\frac{\partial v}{\partial p} - \frac{\partial \varphi}{\partial r} + K_H\left(\frac{\partial^2}{\partial r^2}+\frac{1}{r}\frac{\partial}{\partial r}-\frac{1}{r^2}\right)v + g\frac{\partial \tau_v}{\partial p} \tag{2}$$

$$\frac{\partial \varphi}{\partial p} = -\frac{R\pi}{p}\theta \tag{3}$$

$$\frac{\partial \omega}{\partial p} + \frac{1}{r}\frac{\partial (rv)}{\partial r} = 0 \tag{4}$$

$$\frac{\partial\theta}{\partial t} = -v\frac{\partial\theta}{\partial r} - \omega\frac{\partial\theta}{\partial p} + \frac{Q}{\pi C_p} + K_H\left(\frac{\partial^2}{\partial r^2} + \frac{1}{r}\frac{\partial}{\partial r}\right)\theta + \frac{g}{\pi C_p}\frac{\partial h}{\partial p} \tag{5}$$

where

u = the tangential component of wind
v = the radial component of wind
ω = dp/dt = the p-velocity
θ = the potential temperature
T = $\pi\theta$, the temperature
π = $(p/P_0)^{R/C_p}$, P_0 = 1 000 mb
R = the gas constant of dry air
c_p = the specific heat of air at constant pressure
φ = the geopotential of the isobaric surface
f = the Coriolis parameter
g = the acceleration of gravity
τ_u = the tangential component of vertical stress
τ_v = the radial component of vertical stress
K_H = the coefficient of horizontal eddy viscosity or diffusivity
Q = non-adiabatic heating per unit mass and unit time
h = the vertical eddy flux of sensible heat.

In the present model the horizontal eddy coefficient, K_H, is kept constant and assumes the same value for momentum and heat. The vertical stress terms are assumed to be of the following forms:

$$\tau_u = \frac{1}{g}K_p\frac{\partial u}{\partial p} \tag{6}$$

$$\tau_v = \frac{1}{g}K_p\frac{\partial v}{\partial p} \tag{7}$$

except at the lower boundary. K_p is the vertical eddy coefficient in the p-system. The vertical diffusion of heat in the energy equation is to be neglected in the free atmosphere, and only the heat flux through the lower boundary is taken into account. The non-adiabatic heating term includes only the release of latent heat by condensation which will be discussed in Section 2.4.

2.1. *Gradient balance above the boundary layer*

As discussed in the introduction, the region of concern is divided into two parts: the lower boundary layer, which is taken to be the region below the 900 mb level, and the free atmosphere above the boundary layer. In the free atmosphere the motion is assumed to be in gradient balance, that is, the equation of motion (2) in the radial direction is replaced by

$$u\left(f + \frac{u}{r}\right) = \frac{\partial\varphi}{\partial r} \tag{8}$$

Under the assumptions of hydrostatic equilibrium and gradient balance there exists a relation between the wind and the temperature fields, which is called the thermal wind equation and is obtained by eliminating the geopotential between (3) and (8):

$$\left(f + \frac{2u}{r}\right)\frac{\partial u}{\partial p} = -\frac{R\pi}{p}\frac{\partial\theta}{\partial r} \tag{9}$$

Further, on taking the local time derivative of (9) and substituting the right-hands of (1) and (5) in $\partial u/\partial t$ and $\partial\theta/\partial t$ respectively, we obtain a relation which ω and v must satisfy in order that the tangential wind and the temperature fields are compatible. In terms of the Stoke's stream function ψ, defined in accordance with (4) by

$$-v = \frac{1}{r}\frac{\partial\psi}{\partial p} \tag{10}$$

$$\omega = \frac{1}{r}\frac{\partial\psi}{\partial r} \tag{11}$$

this compatibility condition is given by

$$A\frac{\partial^2\psi}{\partial p^2} + 2B\frac{\partial^2\psi}{\partial r\,\partial p} + C\frac{\partial^2\psi}{\partial r^2} - \frac{4B}{r}\frac{\partial\psi}{\partial p} - \left\{\left(1 - \frac{R}{C_p}\right)\frac{B}{p} + \frac{C}{r}\right\}\frac{\partial\psi}{\partial r} = rD \tag{12}$$

where

$$A = \left(f + \frac{2u}{r}\right)\left(f + \frac{\partial u}{\partial r} + \frac{u}{r}\right) \tag{13a}$$

$$B = -\left(f + \frac{2u}{r}\right)\frac{\partial u}{\partial p} = \frac{R\pi}{p}\frac{\partial\theta}{\partial r} \tag{13b}$$

$$C = -\frac{R\pi}{p}\frac{\partial\theta}{\partial p} \tag{13c}$$

$$D = \frac{\partial}{\partial p}\left\{\left(f + \frac{2u}{r}\right)\left[K_H\left(\frac{\partial^2}{\partial r^2} + \frac{1}{r}\frac{\partial}{\partial r} - \frac{1}{r^2}\right)u + g\frac{\partial \tau_u}{\partial p}\right]\right\}$$

$$+ \frac{R}{pC_p}\frac{\partial}{\partial r}\left\{Q + \pi C_p K_H\left(\frac{\partial^2}{\partial r^2} + \frac{1}{r}\frac{\partial}{\partial r}\right)\theta\right\} \qquad (13\,\mathrm{d})$$

When the tangential wind u, the temperature field θ, and the diabatic heating Q, are given, eq. (12) can be solved for ψ which determines the circulation in the meridional palne, i.e., v and ω through eqs. (10) and (11).

In the present model we choose the system of eq. (1), (9), (10), (11) and (12) as the governing equations of the motion in the free atmosphere. This system, evidently, is self-consistent, compatible with the basic assumptions and closed if Q is formulated in terms of the variables in the system or their boundary values. It is the same system chosen by Sundqvist (1970) except that eq. (12) is applied by Sundqvist to the entire atmosphere but here to the free atmosphere only, and that the continuity equation of moisture is not included here mainly for economic reasons.

2.2. *The explicit boundary layer*

In order to suitably describe the boundary-layer flow field, u and v are calculated at two levels by the primitive equations; one is at 940 mb which approximately represents the average Ekman layer, the other is at the bottom which roughly represents the surface layer. The ω field is then obtained from the continuity equation (4). Thus, at 940 mb level,

$$\frac{\partial u}{\partial t} = -v\left(f + \frac{u}{r}\right) - \frac{1}{r}\frac{\partial}{\partial r}(rvu) - \frac{\partial}{\partial p}(\omega u)$$

$$+ K_H\left(\frac{\partial^2}{\partial r^2} + \frac{1}{r}\frac{\partial}{\partial r} - \frac{1}{r^2}\right)u + \frac{\partial}{\partial p}\left(K_p\frac{\partial u}{\partial p}\right) \qquad (14)$$

$$\frac{\partial v}{\partial t} = \left(f + \frac{u + u_{\mathrm{gr}}}{r}\right)(u - u_{\mathrm{gr}}) - \frac{1}{r}\frac{\partial (rv^2)}{\partial r} - \frac{\partial (\omega v)}{\partial p}$$

$$+ K_H\left(\frac{\partial^2}{\partial r^2} + \frac{1}{r}\frac{\partial}{\partial r} - \frac{1}{r^2}\right)v + \frac{\partial}{\partial p}\left(K_p\frac{\partial v}{\partial p}\right) \qquad (15)$$

where u_{gr} is the gradient wind at the 940 mb level and the transport terms are written in flux forms with the help of (4) for convenience. In order to reduce the small-scale high-frequency oscillations in the boundary layer, we follow the conventional approach which assumes that the pressure gradient remains constant vertically throughout the boundary layer. Thus, u_{gr} is a function of r only and it can be approximated by the tangential wind at the top of the boundary layer. At the bottom, we assumed $\omega = 0$ and hence

$$\frac{\partial u}{\partial t} = -v\left(f + \frac{u}{r}\right) - v\frac{\partial u}{\partial r}$$

$$+ K_H\left(\frac{\partial^2}{\partial r^2} + \frac{1}{r}\frac{\partial}{\partial r} - \frac{1}{r^2}\right)u + F_u \qquad (16)$$

$$\frac{\partial v}{\partial t} = \left(f + \frac{u + u_{\mathrm{gr}}}{r}\right)(u - u_{\mathrm{gr}}) - v\frac{\partial v}{\partial r}$$

$$+ K_H\left(\frac{\partial^2}{\partial r^2} + \frac{1}{r}\frac{\partial}{\partial r} - \frac{1}{r^2}\right)v + F_v \qquad (17)$$

where

$$F_u = -\frac{1}{\delta}\left[g\tau_{us} - \left(K_p\frac{\partial u}{\partial p}\right)_{980\ \mathrm{mb}}\right] \qquad (16\,\mathrm{a})$$

$$F_v = -\frac{1}{\delta}\left[g\tau_{vs} - \left(K_p\frac{\partial v}{\partial p}\right)_{980\ \mathrm{mb}}\right] \qquad (17\,\mathrm{a})$$

and δ is the pressure difference corresponding to the average depth of the surface layer, which we take as 20 mb.

Since the moisture content in the boundary layer is one of the important variables in the formulation of the diabatic heating Q, the specific humidity q is calculated at the bottom and the top of the boundary layer. So is the potential temperature. Near the sea surface, the air is taken as well mixed in the vertical so that the vertical gradients of specific humidity and potential temperature are zero. Here the horizontal eddy diffusion is taken as negligible in comparison with the horizontal advection by the radial wind. The most important diabatic heating and moisture sources are the boundary fluxes from the sea surface. Thus, the specific humidity and the potential temperature at the bottom are given respectively by

$$\frac{\partial q}{\partial t} = -v\frac{\partial q}{\partial r} + \frac{gF_q}{\Delta p} \qquad (18)$$

$$\frac{\partial \theta}{\partial t} = -v\frac{\partial \theta}{\partial r} + \frac{gh_s}{C_p\pi_s}\frac{1}{\Delta p} \qquad (19)$$

where F_q is the moisture flux from the sea surface, h_s the heat flux, p_s the sea-surface pressure, and Δp, a function of the average depth of the Ekman layer, is taken as 50 mb. We require q and T at the bottom to be less than or equal to q_w and T_w respectively, where T_w is the water temperature and q_w is the saturation mixing ratio at T_w and p_s. The surface pressure p_s is obtained by integrating the gradient wind equation (8) with respect to r at the sea surface. When T or q exceeds the above limit, it is adjusted to the limit so that the fluxes of heat and moisture are always from the sea to the air. We note that, in the above boundary layer treatment, the variation of surface pressure is taken into account in computing T_s and q_s, while the depths of the Ekman layer and the surface layer are considered constant.

At the top of the boundary layer the potential temperature is linearly interpolated between the value at the bottom and the value at the 800 mb level, and q is calculated by assuming constant relative humidity in the vertical throughout the boundary layer. It is noted that overestimation may result from these simplifications.

2.3. The boundary conditions

We apply our model to a region which is laterally bounded by $r=0$ and $r=r_{\max}$. Vertically it is bounded below by the sea surface, which is approximated by $p=1\,000$ mb, and bounded above by $p=100$ mb. Above the 100 mb level, the atmosphere is taken as undisturbed.

At the top boundary we assumed zero stress, zero ω and constant potential temperature, i.e.,

$$\tau_u=0,\ \tau_v=0,\ \psi=0 \text{ and } \theta=\text{constant at } p=100 \text{ mb} \tag{20}$$

At the top of the boundary layer, u, θ and ω are continuous. At the lower boundary, the p-velocity is assumed to be zero, and the boundary fluxes of momentum, sensible heat and moisture at the sea surface assume the following conventional forms:

$$\tau_{us}=\varrho C_D Vu \tag{21a}$$

$$\tau_{vs}=\varrho C_D Vv \tag{21b}$$

$$h_s=C_p\varrho C_D V(T_w-T) \tag{21c}$$

$$F_q=\varrho C_D V(q_w-q) \tag{21d}$$

where ϱ is the air density, C_D is the drag coefficient, V is the absolute value of horizontal wind, i.e., $V=(u^2+v^2)^{\frac{1}{2}}$ at the surface.

According to the assumption of axial symmetry, the lateral boundary conditions at the center are zero horizontal gradient of potential temperature and zero wind. Thus,

$$u=0,\ \frac{\partial\theta}{\partial r}=0 \text{ and } \psi=0 \text{ for } r=0 \tag{22}$$

At the outer lateral boundary we assume constant angular momentum. The potential temperature, specific humidity and surface pressure are assumed to remain constant. Thus, we have

$$\frac{\partial\theta}{\partial t}=\frac{\partial q}{\partial t}=\frac{\partial p_s}{\partial t}=0,\ ru=\text{const, for } r=r_{\max} \tag{23}$$

The value of ψ is specified by the following equation:

$$\frac{\partial\psi}{\partial r}=-\frac{\psi}{R^*} \text{ for } r=r_{\max} \tag{24}$$

where R^* is a constant. The same boundary condition was used by Ooyama (1969) and Sundqvist (1970). We take $R^*=1\,800$ km for $r_{\max}=600$ km.

2.4. *Parameterization of the effects of organized cumulus convection*

Concerning the behaviour of the cumulus clouds and their influence and dependence upon the large-scale dynamics, we make use of the following assumptions and simplifications:

(*a*) The total amount of latent heat released in a vertical column of air is specified by the upward flux of water vapor at the top of the boundary layer and hence is given by

$$Q_{\text{total}}=\frac{1}{g}\int_{p_t}^{p_b}Qdp=\begin{cases}-(Lq\omega/g)_{900\,\text{mb}}, & \text{if } \omega_{900\,\text{mb}}<0\\ 0, & \text{otherwise}\end{cases} \tag{25}$$

where p_b and p_t are the levels of cloud base and top respectively, L is the latent heat of condensation.

(*b*) The vertical distribution of the released heat is proportional to the temperature difference between the cumulus clouds and the mean fields, as proposed by Kuo (1965). Thus, let δT denote the temperature difference,

$$Q = \lambda c_p \delta T \tag{26}$$

where

$$\lambda = \frac{Q_{\text{total}}}{c_p(p_b - p_t)\overline{\delta T}} \tag{27a}$$

$$\overline{\delta T} = \frac{1}{(p_b - p_t)} \int_{p_t}^{p_b} \delta T dp \tag{27b}$$

(c) However, when the atmospheric temperature approaches that of the cumulus clouds, the heating assumed the following form instead, as proposed by Sundqvist (1970)

$$Q = \alpha Q_1 + (1 - \alpha) Q_2 \tag{28}$$

where

$$Q_1 = \lambda c_p \delta T \tag{28a}$$

$$Q_2 = Q_{\text{total}}/(p_b - p_t) \tag{28b}$$

$$\alpha = \exp\left(-(\gamma/\overline{\delta T})^2\right) \tag{28c}$$

and γ is a constant. Corresponding to the following way of computing δT, we take 0.4 C for γ.

(d) To calculate the temperature difference δT, we try to include the entrainment effect in a simple manner. Thus, we assume that the rate of entrainment is proportional to $\delta T/T$ which may be interpreted as the divergence of the vertical motion of cloud mass, and δT is computed by the following procedure:

(i) Given temperature, humidity and pressure at sea surface, T_c at 900 mb is determined by a pseudo-adiabatic ascent, and

$$\delta T = \begin{cases} T_c - T, & \text{if } T_c > T \\ 0, & \text{otherwise} \end{cases} \tag{29}$$

(ii) Knowing T_c, T and $\delta T (\geq 0)$ at the level p, we first obtain $\tilde{T}_c$ by subtracting $E\delta T$ from T_c, i.e.,

$$\tilde{T}_c = T_c - E\delta T, \quad E = \mu \delta T/T, \quad \mu = 7.5 \text{ (a non-dimensional constant)} \tag{30}$$

where $E\delta T$ represents the influence of entrainment on T_c. Then we obtain T_c for the level $p - \delta p$ by following the pseudo-adiabat from $\tilde{T}_c$ at p, and compute δT at this level by the same formula (29). This procedure is repeated till a level where $T_c < T$ is reached.

(iii) The highest level with positive δT is taken to be the cloud top p_t. The lowest level with positive δT is taken to be the cloud base; usually we have 900 mb $\geq p_b \geq$ 800 mb. The effect of those cumulus clouds with base higher than the 800 mb level is neglected.

(e) The effect of cumulus clouds on the vertical transport of momentum is included roughly through increasing the eddy-viscosity coefficient in the cumulus-convection regions by an amount proportional to the frictional pumping. Thus,

$$K_p = g^2 \varrho_{st}^2 \times K_z (1 - \beta(\omega q)_{900\,\text{mb}}) \tag{31}$$

where

$$\beta = \begin{cases} \text{a positive constant in cumulus regions} \\ 0, \text{ otherwise} \end{cases} \tag{32}$$

and ϱ_{st} is the standard-atmosphere density. We take 2×10^5 sec/mb for β, which gives a maximum K_p value about twenty times bigger than its value in cumulus-free region.

3. Numerical methods

Since the free atmosphere and the boundary layer are characteristically different, it is natural to adopt different numerical schemes for the solution of the governing equations in the two regions. The free atmosphere is represented by discrete points 100 mb apart vertically and 30 km apart radially. ψ and ω are specified at points where $p = i\delta p$, $i =$ i, ..., 9 and $r = j\delta r$, $j = 0, 1, ..., 20$. u and v are specified at the mid-vertical points where $p = i'\delta p$, $i' = 3/2, 5/2, ..., 17/2$ and $r = j\delta r$, $j = 0, 1, ..., 20$. T is specified at the horizontal mid-points where $p = i\delta p$, $i = 1, 2, ..., 9$ and $r = j'\delta r$, $j' = 1/2, 3/2, ... 39/2$. Forward differencing is used for local time derivatives. Spatial difference is centered. The so-called "box method" difference scheme is employed in the nonlinear transport terms so that nonlinear computational instability is prevented. This scheme is exampled by the following expression of the momentum flux:

$$\left[\frac{1}{r}\frac{\partial}{\partial r}(rvu)+\frac{\partial}{\partial p}(\omega u)\right]_{i+\frac{1}{2},j}=\frac{1}{r_j\delta r}$$

$$\times\left[r_{j+\frac{1}{2}}\frac{v_{i+\frac{1}{2},j+1}+v_{i+\frac{1}{2},j}}{2}\frac{u_{i+\frac{1}{2},j+1}+u_{i+\frac{1}{2},j}}{2}\right.$$

$$\left.-r_{j-\frac{1}{2}}\frac{v_{i+\frac{1}{2},j}+v_{i+\frac{1}{2},j-1}}{2}\frac{u_{i+\frac{1}{2},j}+v_{i+\frac{1}{2},j-1}}{2}\right]$$

$$+\frac{1}{\delta p}\left[\omega_{i+1,j}\frac{u_{i+\frac{1}{2},j}+u_{i+\frac{3}{2},j}}{2}\right.$$

$$\left.-\omega_{i,j}\frac{u_{i+\frac{1}{2},j}+u_{i-\frac{1}{2},j}}{2}\right] \qquad (33)$$

To solve eq. (12) for ψ, several methods including ADI method have been tried. Finally we used an iterative method (which may be called row-by-row sequential relaxation). This method is the most efficient one of those we tried. Eq. (12) is written in the form

$$-a_{ij}\psi^{n+1}_{i,j+1}+2b_{ij}\psi^{n+1}_{i,j}-c_{ij}\psi^{n+1}_{i,j-1}=d_{ij} \qquad (34)$$

where d_{ij} is a function of A, B, C, D, $\psi^n_{i+1,j+1}$, $\psi^n_{i+1,j-1}$, $\psi^n_{i+1,j}$, $\psi^n_{i-1,j+1}$, $\psi^{n+1}_{i-1,j}$ and $\psi^{n+1}_{i-1,j-1}$, ψ^n is the approximation of ψ at the nth iteration. This equation is solved exactly for $i=2, 3, ..., 8$ in each iteration by the method described in Section 8.5 of Richtmeyer & Morton (1967).

In the boundary layer, as mentioned earlier, u and v are calculated at 940 mb and at the bottom, all at $r=j\delta r$, $j=0, 1, ..., 20$, while potential temperature and specific humidity are calculated at the bottom and the top of the boundary layer at $r=j'\delta r$, $j'=1/2, 3/2, ... 39/2$. We use centered difference to approximate all the partial derivatives except that, in order to suppress gravity waves and small-scale noise, we employ upstream differencing for radial partial derivatives in the nonlinear advective terms and the so-called "simulated backward difference" scheme in time integration. The simulated backward difference method may be illustrated by considering the equation

$$\frac{\partial X}{\partial t}=A(X)+F(X)$$

where F is the friction or diabatic heating term, A is the rest excluding friction and heating. The scheme for the solution of X is to repeat the following:

1. given X^n at time step n,
2. $X'=X^n+\delta t(A(X^n)+F(X^n))$,
3. compute boundary values from the boundary conditions,
4. $X^{n+1}=X^n+\delta t(A(X')+F(X^n))$,
5. compute boundary values from the boundary conditions.

This scheme is able to suppress the high frequency modes (Matsuno, 1966).

4. Results of a numerical integration

4.1. *Initial state and parameters*

The initial velocity field assumed is essentially a barotropic vortex with tangential wind given by

$$u(r)=U(r/r_0)\exp(0.5-0.5(r/r_0)^2)$$

where $U=15$ m/sec and $r_0=150$ km. The u values at the bottom, however, are given by $u(r)(1-0.015\,U)$. No radial and vertical velocities are present initially. The initial field of potential temperature, being a function of p only, is taken from Jordan's hurricane season mean data (Jordan, 1958). Air temperature at the bottom surface is independent of radius initially, $T_s=26$°C. Surface specific humidity is also independent of r, $q_s=0.018$. Other constants are: $T_w=27.5$°C, $p_s(r_{max})=$ 1 010 mb, $f=0.5\times10^{-4}$ sec^{-1}, $k_H=5\,000$ m^2 sec^{-1}, $C_D=1.5\times10^{-3}$. K_z assumes zero at 100 mb and increases linearly with decreasing height to a value of 10 m^2 sec^{-1} at 980 mb level.

4.2. *General features of the development of the model tropical cyclone*

The integration was carried out for 104 hours. The model cyclone intensifies with an increasing rate in the developing stage and reaches a peak tangential velocity of 50 m/sec in 68 hours. The rate of intensification compares well with the observations of real tropical cyclones. The deepening of pressure in the surface center, the time variations of the maximum tangential wind and the minimum p-velocity at 900 mb, the variations of radial positions of these extremes, and the warming

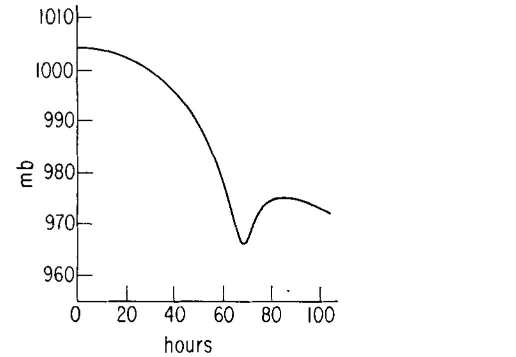

Fig. 1. The time variation of the surface pressure at the center.

up of the core region are shown in Figs. 1–4 respectively.

The variation of minimum surface pressure shown in Fig. 1 indicates a slow dropping from the beginning. In the first 36-hour period the pressure drop is only 7 mb. In the next 24-hour period the pressure drops 19 mb more. The maximum deepening rate over 8 hours is 14 mb, just before the lowest pressure 965 mb occurred. Thereafter, the pressure rises to a value of 975 mb in about 12 hours, and drops again slowly till the end of the computation to a value of 972 mb. It seems that the center pressure undergoes an oscillation after the lowest value is reached.

The maximum tangential wind u_{max} of the model tropical cyclone occurs at 940 mb level. Its time variation, shown in Fig. 2, exhibits a similar nature to that of the surface center pressure. It increases with time almost from the beginning and reaches a peak of 50 m/sec in 68 hours, and then decreases slightly and increases again to a value of about 47 m/sec.

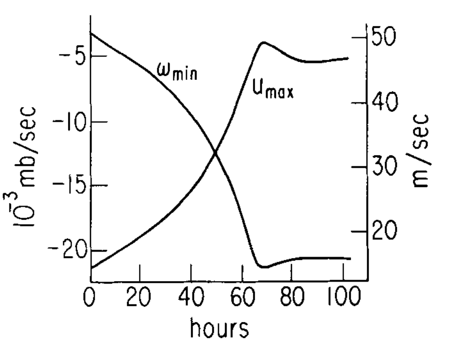

Fig. 2. Time variations of u_{max} and ω_{min}.

The time variation of ω_{min} at 900 mb level is also shown in Fig. 2. The magnitude of ω_{min} represents the maximum rate of pumping air upward through the top of the boundary layer. It also represents the maximum boundary-layer convergence since the p-depth of the boundary layer assumes a constant value and $\omega = 0$ at the bottom surface. It is worthwhile to note that the curves of u_{max} and ω_{min} are just the mirror image of each other except that the peak of the former lags very slightly behind the lowest point of the latter. This fact implies that the boundary-layer pumping is very important to and closely associated with the intensification of the model tropical cyclone. In order to demonstrate the close association between the boundary-layer pumping and the vortex intensification more clearly, the time variations of the radii of u_{max} and ω_{min} are shown in Fig. 3. The radii are determined by fitting each radial distribution of discrete u (or ω) values with a smooth curve. Except during the organization period in the beginning, the resemblance of the two curves in Fig. 3 is indeed remarkable. The radius of u_{max} decreases from 150 km to about 40 km in 66 hours. It then oscillates slightly, approaching a value of 60 km. The radius of ω_{min} is always less than that of u_{max}, i.e., the maximum upward pumping is constantly located inward from the circle of maximum tangential wind, in agreement with the prediction by Kuo (1971) from the vortex boundary layer theory. Except in the organization period, the distance between the two is less than 30 km. The maximum pumping moves inward during the development stage of the model cyclone but never reaches the cyclone center. The smallest radius of ω_{min} is 30 km.

Fig. 4 displays the time variations of the potential temperature anomalies near the cyclone center. The curves A, B and C are plotted

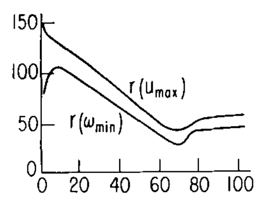

Fig. 3. Time variations of the radii of u_{max} and ω_{min}.

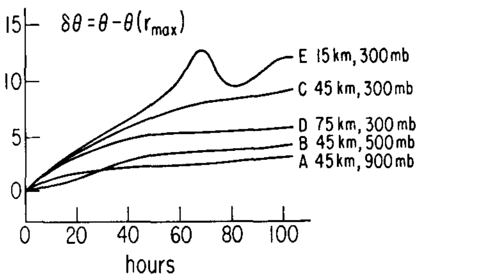

Fig. 4. Time variation of potential temperature anomalies at different locations.

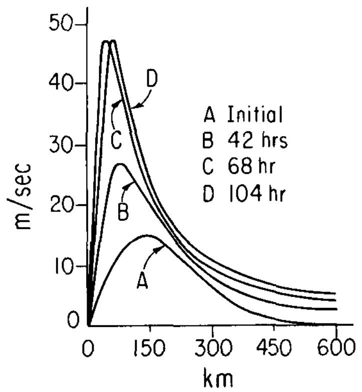

Fig. 5. Radial distribution of the 940 mb tangential velocity at 0, 42, 68, and 104 hours.

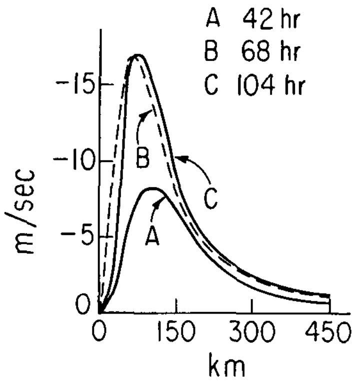

Fig. 6. Radial distribution of the radial velocity at 940 mb.

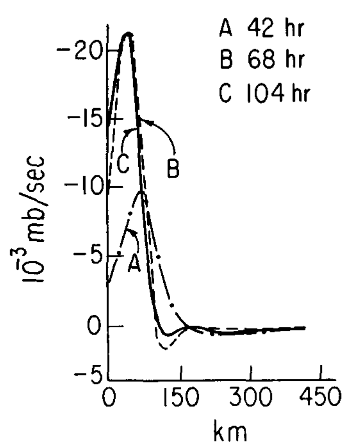

Fig. 7. Radial distribution of ω at 900 mb.

to show the vertical distribution, and D and E are added to show the horizontal gradient. It is clearly seen that the transition to a warm core begins at high altitudes. The warming-up continues and results in a stabilization in the upper part which shifts the maximum heating downward and intensifies the inflow in the boundary layer. The potential temperature anomaly in the center reaches a maximum in 68 hours, as shown by the curve E, and undergoes an oscillation thereafter which is obviously connected with the oscillation in surface presssure shown in Fig. 1, and the slight drop in maximum wind shown in Fig. 2. We note, however, that the temperature gradient from the second grid outward remains unaffected by the oscillation, as revealed by the curves C and D.

The above gross features of our model cyclone generally agree with those of Sundqvist's except that no apparent decaying stage as found by Sundqvist appears in our simulation. Instead of all the facts of continual decaying found by him, such as the outward migration of $\omega_{\min}$, the weakening of the warm core, the rising of the center surface pressure, and the decreasing of the maximum wind, we find a quasi-steady state after a slight oscillation. Ooyama (1969) also found a nearly steady state instead of a decaying stage in his 3-level model. The small oscillation in our results may either be a real phenomenon or it may be due to poor resolution of the model because of the coarse grid near the center, but it is most likely a real occurrence.

In order to see the change of the radial structure during the development of the model cyclone, the radial distributions of u and v at 940 mb, ω at 900 mb and the surface pressure are shown respectively in Figs. 5–8 at 42 hours, 68 hours and 104 hours. At 42 hours the model cyclone just begins its rapid *intensification;*

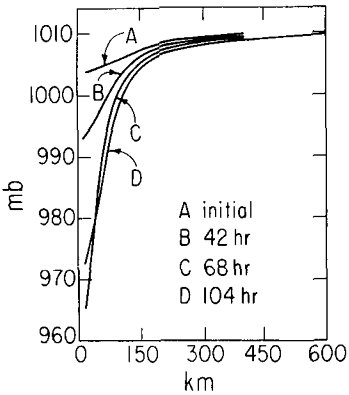

Fig. 8. Surface pressure distribution.

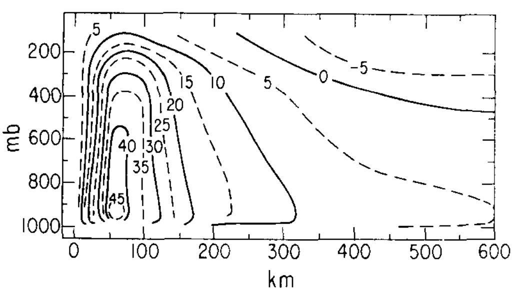

Fig. 9. Vertical cross section of tangential velocity at 104 hours.

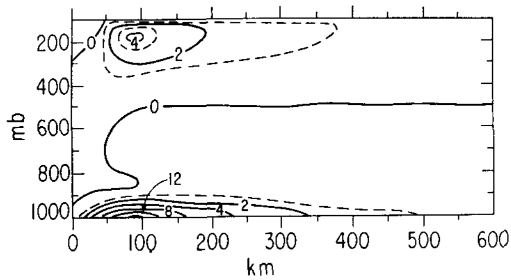

Fig. 10. Vertical cross section of radial velocity at 104 hours.

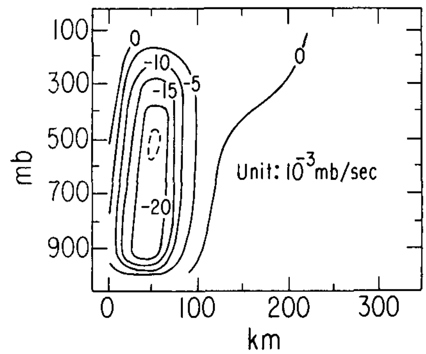

Fig. 11. Vertical cross section of ω at 104 hours.

at 68 hours it becomes fully developed; and at 104 hours the simulation ends. We may regard the period from 42–68 hours as the rapid development stage, and the period from 68–104 hours as the mature or quasi-steady stage. It is clearly seen that in the rapidly developing stage the radii of $u_{\max}$, $v_{\max}$ and $\omega_{\min}$ simultaneously migrate inwards, u and v increase everywhere, most rapidly in the region just inside their respective radii of maximum. The surface pressure decreases everywhere, most rapidly in the center. The vertical velocity increases rapidly inside and near the radius of its maximum, but the area of upward motion contracts, allowing the radius of maximum downward motion also to shift inwards. In the quasi-steady period, the maxima of u and v at 940 mb and the minima of $\omega_{900\,\mathrm{mb}}$ and p_s show only small changes, and the outward shifts of their radii are very slight and can only be detected from the decrease in u or v or the increase in $\omega_{900\,\mathrm{mb}}$ or p_s at the grid next to the center, and from the small intensification outward.

4.3. *The structure of the simulated tropical cyclone*

The vertical cross sections of the tangential, radial and vertical velocities at 104 hours are shown in Figs. 9–11. In general the distribution of the computed tangential velocity (Fig. 9) looks realistic in comparison with observations. The storm winds extend to high altitudes. Weak anticyclonic rotations appear in the upper part of the outer region. Due to the coarse grid near the center, however, the radius of the maximum wind is too large and the concentration around the center is not so pronounced.

The distribution of the radial velocity in Fig. 10 agrees with the expected results. The inflow is concentrated to the boundary layer and the outflow to the uppermost levels. Near the center, a very weak inflow appears at the top. In comparison with Sundqvist's results, our inflow is more confined to the bottom and our radius of maximum inflow is considerably smaller. These are what we expect because Sundqvist did not use a separate boundary layer as we did.

The ω-field shown in Fig. 11 depicts the

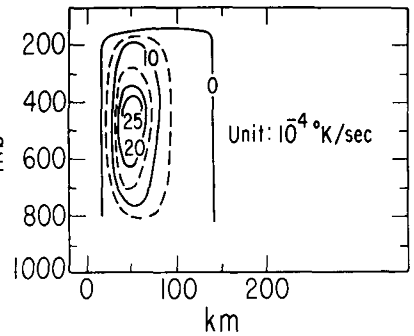

Fig. 12. Vertical cross section of heating rate due to condensation.

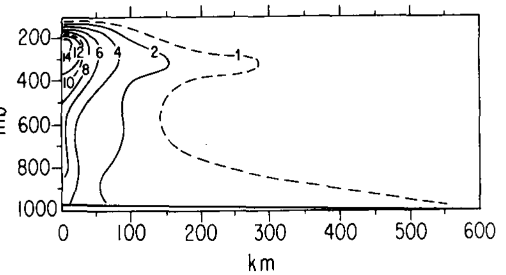

Fig. 14. Vertical cross section of potential temperature anomaly at 104 hours.

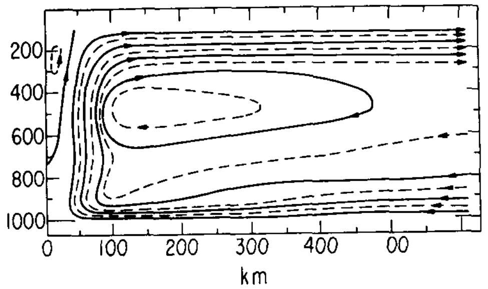

Fig. 13. Stoke's stream function in a meridional plane at 104 hours.

concentration of upward motion to a narrow ring which is just inside the maximum wind belt. It is this strong upward motion that causes the intense diabatic heating shown in Fig. 12. In order to give a clear view of the circulation in a meridional plane, the Stokes' stream function corresponding to Figs. 10 and 11 is shown in Fig. 13. It is apparent that, in contrast to the concentrated upward motion, downward motion prevails almost everywhere outside the 100–200 km radius. We notice also a very weak circulation over the surface center.

Fig. 14 shows the vertical cross section of potential temperature anomalies at 68 hours. The warm-core structure is clearly depicted. Although the heat released by cumulus convection at this time is centered around 500 mb about 50 km away from the cyclone center, the center of net warming is located at about 300 mb in the cyclone center.

5. Concluding remarks

A numerical simulation of the development of a tropical cyclone has been performed with a 10-level axisymmetric model. In this model, the winds in the boundary layer are computed directly from the primitive equations of motion, while in the region above the boundary layer a gradient-wind balance is assumed. The results obtained from a 104 hour integration indicate that the model is capable of simulating the development of a tropical cyclone with a fair degree of reality. Our boundary layer formulation is more similar to that of Ooyama (1969) than to that of Sundqvist (1970). Indeed, instead of the decaying stage obtained by Sundqvist, our results seem to indicte that a quasi-steady state has been achieved as in Ooyama's & Rosenthal's (1970) results. However, although there were real observations which seemed to indicate the possibility of the existence of a steady-state for a given set of parameters, and one might attribute the decay of real tropical cyclones to the change of environmental conditions, it is still hard to say that, after a tropical cyclone reaches its mature stage, a steady-state is closer to reality than a decaying stage if the environmental conditions remain unchanged.

Due to the coarse resolution in the radial direction the eye structure of a typhoon has not been well simulated in our model. A much finer resolution is desired for future work. There are several other simplifications in our model which were made for computational economy, e.g., the omission of humidity calculations above the boundary layer, the omission of cumulus effect on environmental humidity and the simplification in computing temperature and humidity at the top of the boundary layer. These are left for future improvements.

Acknowledgement

This work was suported jointly by NSF under grant NSF GA-25161 and by NOAA under grant N22-154-72(G). The work was performed while the first author was on leave from the National Taiwan University.

REFERENCES

Charney, J. G. & Eliassen, A. 1964. On the growth of the hurricane depression, *J. Atmos. Sci. 21,* 68–75.

Jordan, C. L. 1958. Mean soundings for the West Indies area. *J. Meteor. 15,* 91–97.

Kasahara, A. 1961. A numerical experiment on the development of a tropical cyclone. *J. Meteor. 18,* 259–282.

Kuo, H. L. 1961. Convection in conditionally unstable atmosphere. *Tellus 13,* 441–459.

Kuo, H. L. 1963. On formation and intensification of tropical cyclones by deep cumulus convection. *Geofisica Internacional (Mexico) 4,* 199–205.

Kuo, H. L. 1965. On formation and intensification of tropical cyclones through latent heat release by cumulus convection. *J. Atmos. Sci. 22,* 40–63.

Kuo, H. L. 1971. Axisymmetric flows in the boundary layer of a maintained vortex. *J. Atmos. Sci. 28,* 20–41.

Kuo, H. L. 1974. Further studies of the parameterization of the influence of cumulus convection on large-scale flow. *J. Atmos. Sci. 31,* 1232–1240.

Matsuno, Y. 1966. Numerical integrations of primitive equations by use of a simulated backward difference method. *J. Meteor. Soc. Japan 44,* 76–84.

Ooyama, K. 1964. A dynamic model for the study for tropical cyclone development. *Geofisica Internacional (Mexico) 4,* 187–198.

Ooyama, K. 1969. Numerical simulation of tropical cyclones with an axisymmetric model. Proc. of WMO/IUGG Symposium on Numerical Weather Prediction in Tokyo, 1968, III, pp. 81–88, Japan Meteor. Agency, 1969.

Richtmyer, R. D. & Morton, K. W. 1967. *Difference methods for initial-value problems.* Wiley, New York, pp. 405.

Riehl, H. & Malkus, J. S. 1961. Some aspects of Hurricane Daisy, 1958. *Tellus 13,* 181–213.

Rosenthal, S. 1970. A survey of experimental results obtained from a numerical model designed to simulate tropical cyclone development. ESSA Tech. Memo. ERLTM-NHRL *88,* 74 pp.

Rosenthal, S. 1973. Hurricane modeling experiments with a new parameterization for cumulus convection, NOAA Technical Mem. ERL WMPO-4, 41 pp.

Sundqvist, E. H. 1970. Numerical simulation of the development of tropical cyclones with a ten-level model, Part I. *Tellus 22,* 359–390.

Yamasaki, M. 1968. Detailed analysis of a tropical cyclone simulated with 13-level model. *Papers in Meteor. and Geophys. 19,* 559–585.

Yanai, M. 1961. A detailed anslysis of typhoon formation. *J. Meteor. Soc. Japan 39,* 187–213.

ЧИСЛЕННОЕ МОДЕЛИРОВАНИЕ РАЗВИТИЯ ТРОПИЧЕСКОГО ЦИКЛОНА

С помощью 10-уровенной осесимметричной модели выполнен численный эксперимент для изучения развития тропических циклонов. В этой модели ветер в пограничном слое вычисляется непосредственно из примитивных уравнений движения, но выше пограничного слоя подразумевается градиентный баланс. Вклад мощных кучевых облаков в нагревание крупномасштабного их окружения параметризуется согласно идеям Куо (1965) и Сандквиста (1970). Грубым образом учитывается также вклад кучевых облаков в вертикальный перенос количества движения. Эксперимент показывает, что данная модель способна описать многие особенности реально наблюдаемых тропических циклонов. Наши результаты отличаются от результатов Сандквиста (1970) в одном важном аспекте, именно, у нас не происходит быстрого затухания циклона после развитой стадии, если внешние условия и параметры остаются неизменными, что согласуется с результатом Оояма (1969). Довольно детально обсуждаются процесс развития и структура моделируемого тропического циклона.